THE ASTROPHYSICAL JOURNAL, 468:532–542, 1996 September 10

THE HEAD-ON COLLISION BETWEEN TWO GAS-RICH GALAXIES: NEUTRAL HYDROGEN DEBRIS FROM THE CENTRALLY SMOOTH RING GALAXY VII Zw 466

P. N. APPLETON,[1] V. CHARMANDARIS,[1,2] AND C. STRUCK
Department of Physics and Astronomy, Iowa State University, Ames, IA 500 11
Received 1995 December 18; accepted 1996 April 4

ABSTRACT

We present VLA observations of the distribution and kinematics of the H I gas in the classical ring galaxy VII Zw 466 and its immediate surroundings. The H I gas corresponding to the bright optical star forming ring exhibits the typical profile of a rotating-expanding ring. The systemic velocity of the galaxy is found to be 14,468 ± 25 km s^{-1}. A formal fit to the H I kinematics in the ring is consistent with both ring rotation and expansion (expansion velocity 32 km s^{-1}). However, H I in the northeast quadrant of the ring is severely disturbed, showing evidence of tidal interaction. In addition, fingers of H I gas extend from the galaxy to the east in the general direction of the two major companions. We also detect a hydrogen plume from the southern edge-on companion galaxy (G2) pointing toward the ring galaxy. This, and other peculiarities associated with G2 suggest that it is the intruder galaxy which recently collided with VII Zw 466 and formed the ring. Numerical hydrodynamic models are presented that show that most of the observed features can be accounted for as a result of the impact splash between two gas disks. The resultant debris is stretched by ring wave motion in the bridge and later forms accretion streams onto the two galaxies.

Finally, we detect H I emission from two previously unknown dwarf galaxies located northeast and southeast of VII Zw 466, respectively. This brings the total number of members of the VII Zw 466 group to five. Using the projected mass method, the upper limit of the dynamical mass of the group was estimated to be $M_0 = 3.5 \times 10^{12}\ M_\odot$, which implies that the mass-to-light ratio of the group is $(M/L)_{\rm group} \approx 70$. This rather low value of M/L, as compared with other loose groups, suggests the group may be in a state of collapse at the present time. Plunging orbits would naturally lead to an enhanced probability of head-on collisions and ring galaxy formation.

Subject headings: galaxies: clusters: individual (VII Zw 466) — galaxies: individual (VII Zw 466) — galaxies: interactions — galaxies: kinematics and dynamics — hydrodynamics — radio lines: galaxies

1. INTRODUCTION

The idea that galaxies might be transformed as a result of interactions, collisions, and mergers was presented by Toomre & Toomre (1972) to explain the diversity of forms seen in many of the images of peculiar galaxies (Arp 1966; Vorontsov-Velyaminov 1977). Observations since that time have further strengthened the view that interactions play a crucial role in galaxy evolution. In particular, as Toomre has suggested, they may be responsible for the formation of elliptical galaxies through major mergers and collisions. Observations of rich clusters of galaxies at redshifts of between 0.3 and 0.6 seem to show an increased fraction of blue galaxies, with a significant fraction undergoing an interaction (Butcher & Oemler 1984; Lavery & Henry 1988; Dressler et al. 1994). For those blue galaxies that are interacting, there is increasing evidence from *HST* observations that many have shell-like or ringlike morphologies (Lavery et al. 1996; Oemler 1996). Although these may not all be collisional systems, it is interesting to study low-redshift galaxies that show similar morphologies and ask whether these are simply analogs of processes occurring at higher redshift. In this category we would include the shell ellipticals (Malin & Carter 1980), the galaxies with ripples (Schweizer & Seitzer 1988) and the collisional ring galaxies (Lynds & Toomre 1976; see Appleton & Struck-Marcell 1996, hereafter AS96, for review).

The collision of two gas-rich disk systems of unequal mass ratio is probably one of the most challenging problems in numerical modeling today (Barnes & Hernquist 1992; Struck 1996a). The treatment of shocks in the disks of two interpenetrating galaxies is quite difficult to simulate and very few examples exist in the literature. Struck (1996b) has recently attempted to model both the hot and cold gaseous component during a head-on collision to produce the Cartwheel ring galaxy and many complicated physical processes are at work during and shortly after the penetration of the "target" galaxy by the "intruder." It is, therefore, of considerable interest to map the cool and hot components of the gas in a real collision and make comparisons with models.

The ring galaxy VII Zw 466 was discussed very early on in the debate about the origin of these peculiar rings (Freeman & de Vaucouleurs 1974; Theys & Spiegel 1976; Lynds & Toomre 1976). An early photometric study of VII Zw 466 was made by Thompson & Theys (1978) in which the colors and knots within the ring were investigated. This galaxy has also been the subject of a recent optical and infrared study (Marston & Appleton 1995; Appleton & Marston 1995) and strong radial color gradients were found within the ring.

[1] Visiting astronomer at NRAO. The National Radio Astronomy Observatory is a facility of the National Science Foundation operated under cooperative agreement by Associated Universities, Inc.

[2] Now at CEA-CEN Saclay, Service d'Astrophysique, 91191 Gif-sur-Yvette Cedex, France.

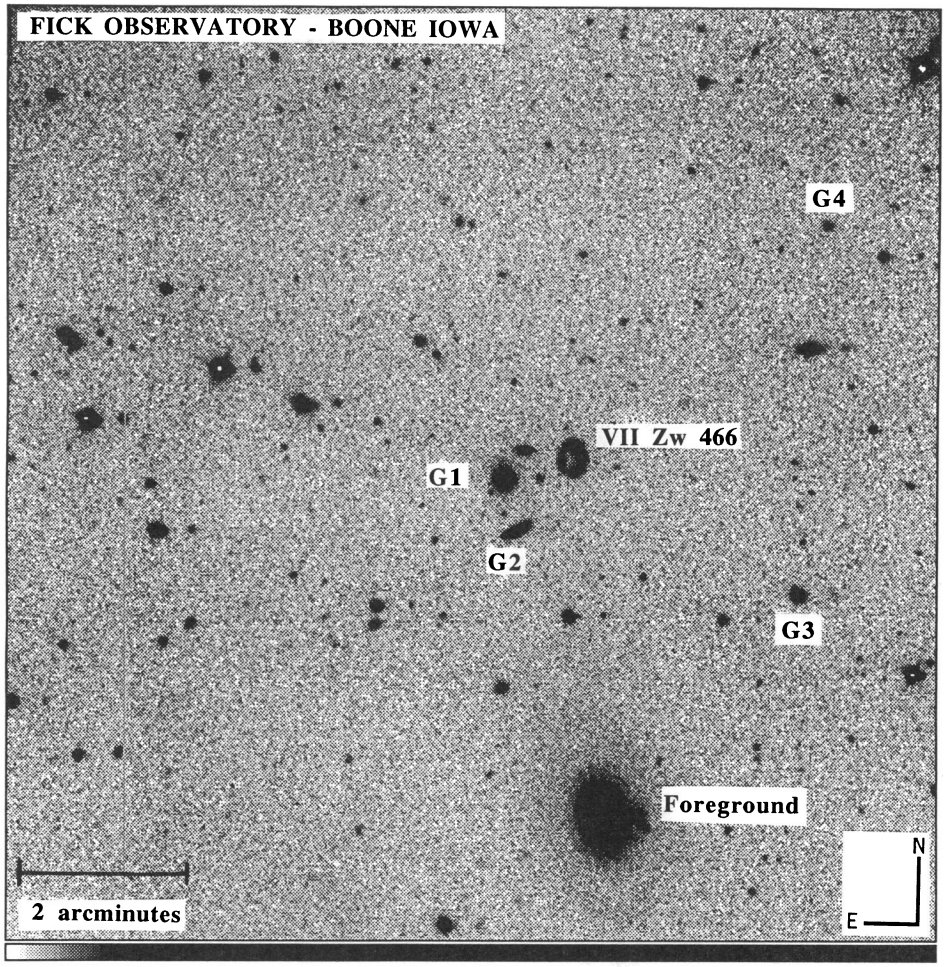

FIG. 1.—Gray-scale image of VII Zw 466 through a V-band filter taken at Fick Observatory. The positions of the two newly discovered dwarfs are marked as G3 and G4.

Throughout this paper, we will adopt a Hubble constant of 80 km s^{-1} Mpc^{-1}. We have determined the heliocentric optical velocity of the galaxy to be 14,468 km s^{-1} and therefore assume a distance to the VII Zw 466 group of 180 Mpc.

2. OBSERVATIONS

The observations were made on 1994 December 3 using all 27 telescopes in the C configuration of the VLA.[3] The correlator was set in a two IF (intermediate frequency) mode (AC BD) with on-line Hanning smoothing and 32 channels per IF. For each IF we used a bandwidth of 3.125 MHz. This provided a frequency separation of 97.6 kHz per channel, which corresponds to 22.66 km s^{-1} in the rest frame of the galaxy using the optical definition of redshift. To achieve a wider velocity coverage, IF1 was centered at 14,131 km s^{-1} and IF2 at 14,538 km s^{-1}. As a result, the velocity coverage of our observations was 974 km s^{-1}. A total of 4 hr 47 minutes was spent on source. Flux and phase calibration was performed using the sources 3C 286 and 01311+678 (B1950), respectively.

These data were first amplitude and phase calibrated and bad data due to interference were flagged and ignored by the AIPS software. An image cube was created from the UV data by giving more weight to those baselines that sampled the UV plane more frequently (so-called natural weighting). This provided a synthesized beam with a FWHM of 23.″3 × 21.″9 for IF1 and 21.″6 × 19.″3 for IF2.

The subtraction of the continuum emission in each line map was performed using a standard interpolation procedure based on four continuum maps free from H I at each end of the band. The resulting rms noise per channel was 0.27 mJy $beam^{-1}$. The highest dynamic range in any channel map was 5:1 (at v = 14,402.8 km s^{-1}) with a peak flux of 1.35 mJy $beam^{-1}$.

In order to determine the total H I distribution we used the following technique. Initially, we smoothed all channel maps to a resolution 44.″0 × 44.″0, twice that of the synthesized beam. New maps were formed comparing, pixel for pixel, the original full resolution maps to the smoothed ones. The pixel values of original maps were copied to the new ones only if the signal-to-noise ratio of the smoothed map at that point exceeded 2. The total H I surface density map was produced by adding the new maps together. The same technique was used to create the first and second moment maps of the distribution. Using this procedure we effectively give more weight to points associated with low surface brightness emission.

Optical observations of a 16′ × 16′ field were obtained during photometric conditions on 1995 April 2, with the Fick Observatory 0.6 m telescope and CCD system (Appleton, Kawaler, & Eitter 1993). A 500 s exposure using an R-band filter was taken. Calibration of the photometry

[3] The Very Large Array is operated by Associated Universities, Inc., under cooperative agreement with the National Science Foundation.

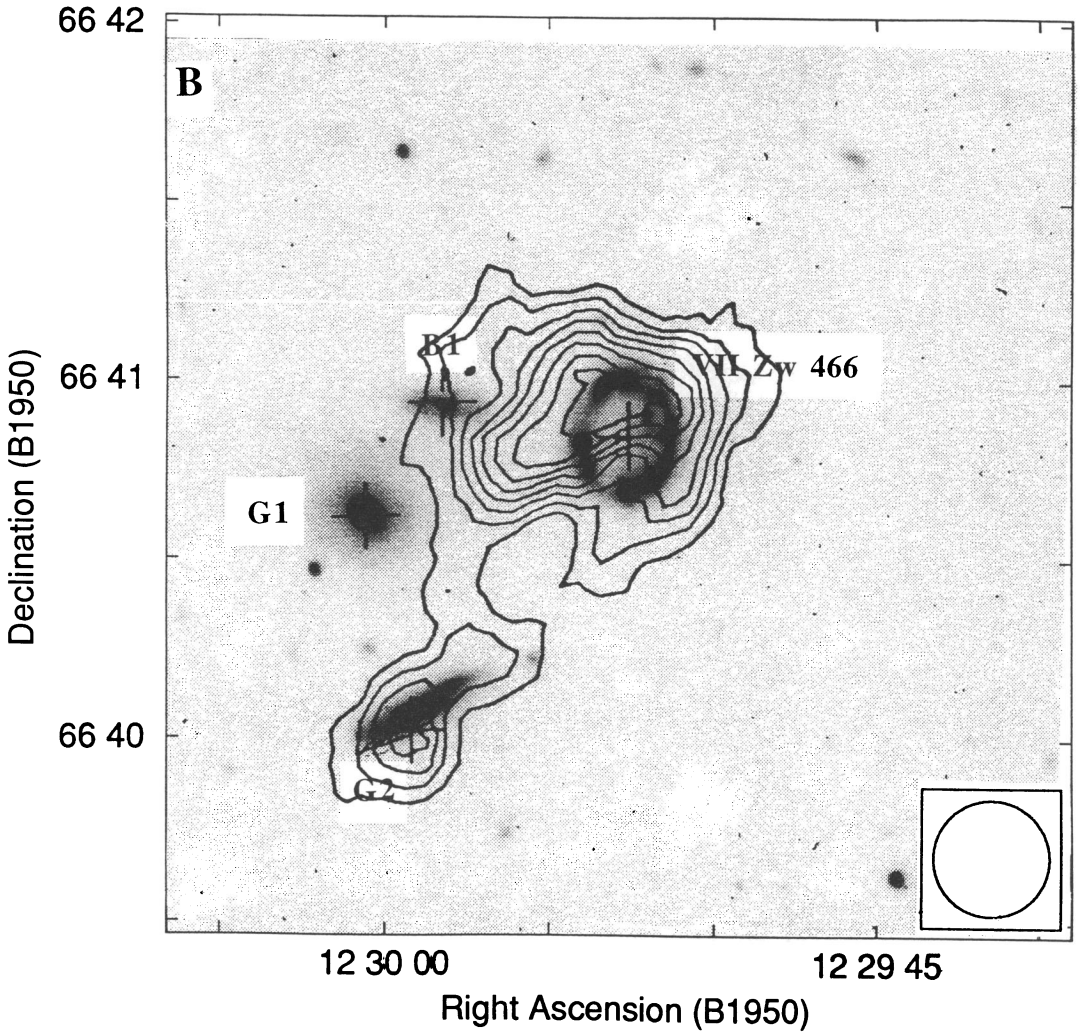

FIG. 2.—Gray-scale image of VII Zw 466 through a *B*-band filter overlayed with a contour map of the integrated H I distribution. The contour increment is 57.15 Jy beam^{-1} m s^{-1}, and the level of the first contour is also 57.15 Jy beam^{-1} m s^{-1}.

was performed using data taken from the star G10 50 (Landolt 1992).

3. THE VII Zw 466 GROUP AND ITS H I DISTRIBUTION

In Figures 1 and 2 we show the VII Zw 466 group and its environment. The ring has two nearby companions, labeled G1 and G2 as well as a background galaxy B1 (Appleton & Marston 1995). Galaxy B1 (first noted as background by R. Lynds; see Theys & Spiegel 1976) has a velocity of $V_{\odot}$ = 25,042 km s^{-1}, determined from our own unpublished optical spectra. Also marked in Figure 1 are two new dwarf galaxies, G3 and G4, discovered during the H I mapping of the group, presented in this paper.

In Figure 2 we show the integrated neutral hydrogen emission from the VII Zw 466 field superimposed on a *B*-band image of the group (from Appleton & Marston 1995). The emission from the ring galaxy is highly disturbed. The brightest emission comes from the northern quadrant of the ring and sweeps around in a clockwise direction along the western quadrant of the ring. A filament of H I extends from the ring in a southeasterly direction, pointing to a region between G1 and G2. In addition, there is a marked depression in the H I emission from the southeastern quadrant of the ring. It is in this quadrant that the optical emission in the ring is rather faint. The H I distribution in VII Zw 466 is similar to that seen by Higdon (1993; 1996) in the Cartwheel ring galaxy, with scattered H I extending in the direction of the three possible companions. As with VII Zw 466, the Cartwheel plumes are highly asymmetric, with all the gas outside the galaxies being found on one side of the ring, highly suggestive of a hydrodynamic splash resulting from the gas-on-gas collision between the galaxies.

H I emission is also detected from the edge-on companion G2. The H I has a large peak centered on the southeastern end of the major axis with fainter emission extending along the major axis. A very faint filament extends from G2 back toward the ring.

No emission down to a level of 0.68 mJy beam^{-1} (2.5 σ) was detected from the peculiar elliptical galaxy G1. If we adopt a typical velocity width of 300 km s^{-1} for the assumed velocity of any gas in the elliptical galaxy, this limit translates into a 2.5 σ upper limit of 3.1 $\times$ 10^9 $M_{\odot}$ for the hydrogen mass of the companion.

We also detected gas from two new group members G3 and G4 located 3.2 and 4.2 to the southwest and northwest

TABLE 1

PROPERTIES OF THE VII ZW 466 GROUP

Property	VII Zw 466	Elliptical (G1)	Spiral (G2)	Dwarf 1 (G3)	Dwarf 2 (G4)
α(J2000).....	12 32 05.27	12 32 13.30	12 32 11.95	12 31 37.99	12 31 35.11
δ(J2000).....	+66 24 13 65	+66 23 59 80	+66 23 19.92	+66 22 35.56	+66 26 55.26
$V_{\rm H\,I}$ (km s^{-1})	14,468 $\pm$ 25	[14,100][a]	14,457 $\pm$ 25	14,046 $\pm$ 25	14,223 $\pm$ 25
$\Delta V_{1/2}$ (km s^{-1}).....	202	...	84	113	25
$\Delta V_{1/5}$ (km s^{-1}).....	256	...	119	...	40
$R_{\rm H\,I}$ (arcsec)	11	...	6.7	9.3	4.6
$\int S(v)dv$[b]	0.541	$\leq$0.408[c]	0.155	0.383	0.092
$M_{\rm H\,I}/M_\odot$[d]	4.1×10^9	$\leq 3.1 \times 10^{9}$[c]	1.2×10^9	2.9×10^9	7.0×10^8
R-band mag.[e]	14.94	14.64	15.62	16.18 $\pm$ 0.05	17.67 $\pm$ 0.10
M_d[f] ($M_\odot$).....	4.10×10^{10}	3.00×10^{11}	2.31×10^9	1.16×10^{10}[g]	1.80×10^{8}[g]
L_R ($L_\odot$)	1.6×10^{10}	2.0×10^{10}	8.2×10^9	4.9×10^9	1.3×10^9
$M_{\rm H\,I}/L_R$ ($M_\odot/L_\odot$).....	0.26	$\leq$0.16	0.14	0.59	0.56
M_d/L_R ($M_\odot/L_\odot$)	2.59	15	0.28	2.36	0.21

NOTE.—Units of right ascension are hours, minutes, and seconds, and units of declination are degrees, arcminutes, and arcseconds.

[a] Optical velocity from Theys & Spiegel 1976.

[b] Where $\int S(v)dv$ is the integrated flux density in Jy km s^{-1}.

[c] Assumes a hypothetical velocity width of 300 km s^{-1} and a solid angle equal to two VLA beams.

[d] Where $M_{\rm H\,I}/M_\odot = D^2 \times 2.356 \times 10^5 \int S(v)dv$ and D = 180 Mpc.

[e] From Appleton & Marston 1995.

[f] $M_d = [0.5\Delta V_{1/2}\ \mathrm{cosec}\ (i)]^2 R_{\rm H\,I}/G$ is an estimate of the total dynamical mass of the galaxy.

[g] Since the dwarf was unresolved from the B-band image, we assumed an inclination $i = 45°$.

of VII Zw 466, respectively. At the distance of the group these correspond to projected linear separations of 166 kpc and 220 kpc from the ring.

4. INTEGRATED PROPERTIES

In Table 1 we present the H I and optical properties of VII Zw 466, its two major companions (G1 and G2), and the two newly discovered dwarf galaxies, G3 and G4. The R-band luminosities, L_R, of G1 and G2 are from Appleton & Marston (1995), while the optical properties of G3 and G4 were determined from the Fick CCD images. There is excellent agreement between the photometry of the galaxies in common between the previously published KPNO magnitudes and the Fick magnitudes.

The velocity profiles of the neutral hydrogen distribution of VII Zw 466, G2, and two dwarfs are presented in the Figures 3, 4, 5, and 6. The H I profile of VII Zw 466 presents the typical two-horned profile of a rotating disk. We estimate the systemic velocity of the ring to be 14,468 $\pm$ 25 km s^{-1}, in close agreement with the optically determined velocity of 14,490 km s^{-1} (Theys & Spiegel 1976). However, the high-velocity horn is not completely symmetrical. Emission seen at velocities higher than 14,520 km s^{-1} is associated with the gas plumes outside of the visible galaxy.

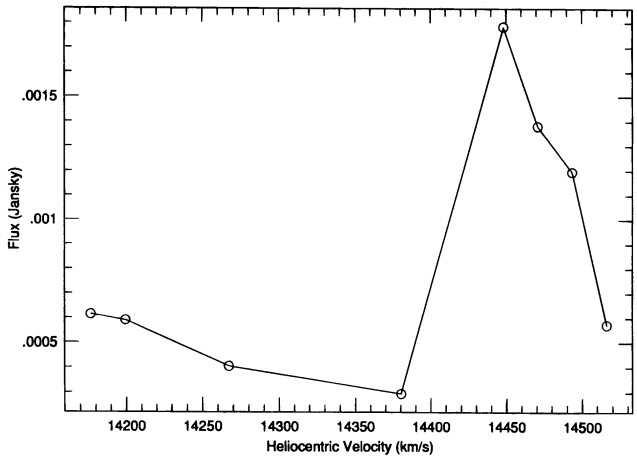

FIG. 4.—Global H I profile of the companion galaxy G2

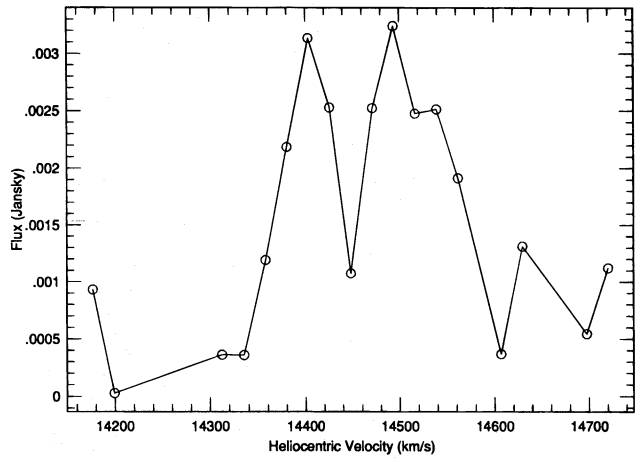

FIG. 3.—The global H I profile of VII Zw 466

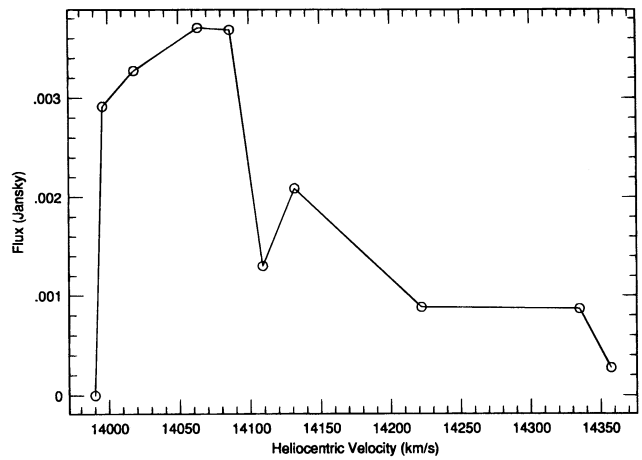

FIG. 5.—Global H I profile of the dwarf galaxy G3

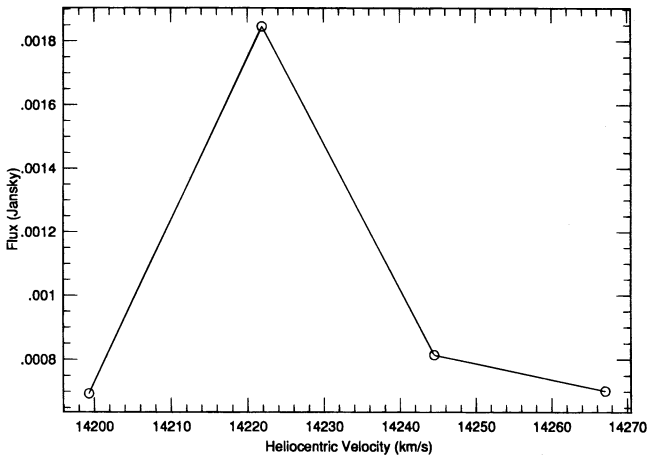

FIG. 6.—Global H I profile of the dwarf galaxy G4

The H I profile of G2 is single-peaked with $\Delta V_{1/2} = 84$ km s^{-1}. The galaxy appears to be edge-on, so for all calculations we used an inclination $i = 90°$. The two dwarfs, though, have more peculiar H I profiles. The velocity profile of G3 exhibits a low-level asymmetry around 14,100 km s^{-1}, which may not be real. For this reason, we did not attempt to calculate $\Delta V_{1/5}$ for this galaxy. Finally, G4, the least massive galaxy in the group, has a very narrow H I profile with $\Delta V_{1/2} = 25.3$ km s^{-1}. For both G3 and G4 we assumed an inclination of $i = 45°$, since the disks of the galaxies were only marginally resolved in the optical images of the group.

We also include in Table 1 a rough estimate the dynamical mass M_d of each group member. The values of M_d corresponding to the galaxies G2, G3, and G4 were calculated using the formula

$$M_d = \frac{[(1/2)\Delta V_{1/2} \text{ cosec } (i)]^2 R_{\text{H I}}}{G},$$

which assumes that the gas is in bound circular orbits. Values of the H I radius were obtained by inspection of the run of emission centroid with radius for each galaxy and in all cases the H I disks were resolved and a radius determined.

The estimate of the dynamical mass of VII Zw 466 was produced by the fit to the rotation of the H I ring discussed in § 6. For completeness, the dynamical mass of G1 was simply estimated from its observed luminosity, using an R-band mass-to-light ratio of $M/L = 15$, typical of elliptical galaxies (Faber & Jackson 1976). Finally, we present the mass-to-light ratio M_d/L_R of G2, G3, G4, and VII Zw 466. We note the surprising small values of M_d/L_R as well as $M_{\text{H I}}/L_R$ for the spiral galaxy G2. We believe that this may be related to the tidal stripping of its mass. We will elaborate more on that in §§ 6 and 8.

5. THE DYNAMICAL MASS OF THE VII Zw 466 GROUP

Our observations indicate that there are now four galaxies G1–G4 that form a loose group around VII Zw 466. Since we know the recession velocities of those galaxies and their angular separations, we can use a dynamical method to get an independent estimate on the total mass of the group and, subsequently, its dark matter content. This is the first time that the large-scale matter content of a group containing a ring galaxy has been estimated.

The primary method used is the *projected mass estimator* proposed by Bahcall & Tremaine (1981). However, for comparison we also estimated the mass of the group using a mass-weighted virial theorem approach. Both give similar results.

The projected mass method is based on the idea that, for a dynamically bound system with one massive object and several smaller companions, one can examine two extreme cases for the possible orbital types of the group members. The first case assumes an isotropic distribution in the velocities of the members, which implies that the average value for the eccentricity of the orbits is $\langle e^2 \rangle = \frac{1}{2}$. The other extreme is that all orbits of the group members are radial implying that $\langle e^2 \rangle = 1$. These lead us to define two specialized estimators of the dynamical mass:

$$M_I = \frac{16}{\pi G N} \sum_{i=1}^{N} v_{zi}^2 R_i ,$$

and

$$M_R = \frac{32}{\pi G N} \sum_{i=1}^{N} v_{zi}^2 R_i ,$$

where v_{zi} is the difference in the recessional velocity between the group member i and the central massive object and R_i is its projected distance from the central object (see Bahcall & Tremaine 1981 for details).

When one has no specific information on the distribution of the eccentricities of the group one can use a dynamical mass estimator that is the average of the two extremes, that is,

$$M_o = \frac{1}{2}(M_I + M_R) = \frac{24}{\pi G N} \sum_{i=1}^{N} v_{zi}^2 R_i .$$

In the VII Zw 466 group the most massive object is the elliptical galaxy G1. However, since its velocity is poorly determined (no H I detection) and its mass is inferred from its luminosity and an assumed mass-to-light ratio, we decided to use the barycentric velocity and position of the group as the point of reference rather than G1. Using the figures presented in Table 1, we find that the barycenter is located at $\alpha_{cm} = 12^{\text{h}}32^{\text{m}}11\overset{\text{s}}{.}2$ and $\delta_{cm} = +66°23'58\overset{''}{.}51$ (J2000) and its systemic velocity is $v_{cm} = 14{,}143$ km s^{-1}. The new position for the center lies only 1 Galactic radius away from the elliptical (the elliptical still dominates). Our results for the mass of the group are presented in Table 2.

Although the use of the barycenter rather than a single galaxy as the center may seem to contradict the assumption that the group is dominated by a single central massive

TABLE 2

PARAMETERS FOR THE DYNAMICAL MASS FOR THE VII Zw 466 GROUP

Galaxy	R_i[a] (kpc)	v_{zi}[b] (km s^{-1})	$q_i = R_i v_{zi}^2/G$ ($M_\odot$)
VII Zw 466.....	33.7	325	8.00×10^{11}
G1.....	11.0	−43	4.57×10^{9}
G2.....	33.9	314	7.51×10^{11}
G3.....	188.4	−97	3.98×10^{11}
G4.....	244.1	80	3.51×10^{11}

[a] Projected distance from the barycenter.
[b] Velocity offset from the systemic velocity of the barycenter ($v_{cm} = 14{,}143$ km s^{-1}).

object, we feel that this is a compromise position, given the poorly determined optical velocity of G1. If the group is dominated by dark matter, then the barycenter of the group might be more appropriate anyway. We note for comparison that had we used G1 as the center, our estimate of the dynamical mass would only be greater by a factor of 1.83 than the result presented in Table 2.

The estimate of the total dynamical mass of the group is $M_o = 3.5 \times 10^{12}\ M_\odot$. The sum of the dynamical masses of each individual (ith) galaxy from Table 1 is

$$M_T = \sum_{i=1}^{5} M_{di} = 3.55 \times 10^{11}\ M_\odot\ ,$$

which implies that the amount of dark matter distributed outside the members of the group is

$$\frac{M_o}{M_T} \approx 9.9\ .$$

Table 1 also shows that the total luminosity of the group is $L_{RT} = 5.02 \times 10^{10}\ L_\odot$, implying that the total mass-to-light ratio for the group is $(M/L)_{\rm group} \approx 70$.

For completeness we also calculated the mass of the group using a method based on the mass-weighted virial theorem. In this approach the mass of the group is given by the formula

$$M_{VT} = \frac{3\pi}{2G} \frac{\sum_{i=1}^{5} M_{di} v_{zi}^2}{\sum_{i=1}^{5} \sum_{j=1,j>i}^{5} (M_{di} M_{dj}/r_{ij})} \left(\sum_{i=1}^{5} M_{di} \right),$$

where M_{di} is again the dynamical mass of a group member i and r_{ij} is the projected distance between the members i and j. This results to a group mass $M_{VT} = 6.2 \times 10^{12}\ M_\odot$, which is only 1.78 times larger than the projected mass method estimate.

We believe that the projected mass method estimate is more accurate than the one resulting from the virial theorem technique. Bahcall & Tremaine (1981) have shown through numerical simulations that the virial theorem technique may be biased and inefficient in particular for systems with small number of members. In addition, the projected mass method has the added advantage that it explicitly takes into account the possibility that some or all of the orbits in the group are radial. The latter reason is very relevant in this study. Unlike most group studies, we know that in the VII Zw 466 group at least two of the galaxies (perhaps G2 and VII Zw 466) must have collided radially in order to produce the ring.

The projected mass method and the virial mass method are valid only if the group is gravitationally bound. If some of the galaxies are leaving the group, or are chance projections of foreground or background galaxies, or the group is not stable, then the resulting dynamical mass and group crossing times would be incorrect.

Other studies of loose groups of galaxies (e.g., Ramella, Geller, & Huchra 1989) show that they have a typical $(M/L) \approx 150$–300, while in compact groups $(M/L) \approx 50$ (Hickson et al. 1992). In some scenarios, it is believed that compact groups are continuously forming at the center of rich loose groups and are in a state of collapse. The fact that the mass-to-light ratio of the VII Zw 466 group is similar to that of compact groups and also the presence of a least one observed collisional ring galaxy pair in the group, suggests that, like the compact groups, VII Zw 466 group may also be collapsing.

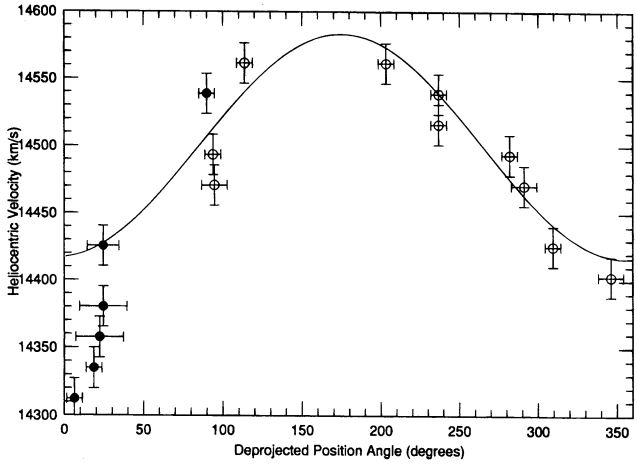

FIG. 7.—H I velocity as a function of azimuth around the ring. The solid circles were excluded from the fit.

6. THE H I KINEMATICS OF THE RING

In order to understand the kinematical behavior of the H I gas in the ring of VII Zw 466, we used a model that assumes that the ring may be both rotating and expanding. This model has been used successfully in other ring galaxies, such as the Cartwheel (Fosbury & Hawarden 1977; Higdon 1993). Using the optical B-band image of the group and assuming an intrinsically circular ring,[4] we estimated the inclination of the ring to be $i = 37°$ and the position angle of the major axis to be $-5°$ (N through E). Then, we measured the velocities of the H I gas along azimuth of the ring and performed a three-parameter fit using the following function:

$$v = a_0 + a_1 \sin(\phi + \phi_0)\ , \qquad (1)$$

where a_0, a_1, and ϕ_0 were the free parameters. A rotating and expanding ring would exhibit a simple sinusoidal shape, with a phase offset from the major axis that is related to the amplitude of the expansion. The formal fit for the ring resulted in a $\chi^2 = 5.61$. However, the points of the northeast quadrant of the ring exhibit a peculiarity related to one of the H I plumes, and the errors associated with them are larger. If we exclude those points (which is reasonable since we are only trying to model the ring), the fit improves considerably, giving a $\chi^2 = 2.77$ for $a_0 = 14{,}500$ km s^{-1}, $a_1 = 83$ km s^{-1}, and $\phi_0 = 274°$. This fit is presented in Figure 7. The azimuthal component of the velocity at the ring radius and the radial expansion velocity, corrected for inclination are found to be $v_{\rm max} = 137$ km s^{-1} and $v_{\rm exp} = 32$ km s^{-1}. We note that this expansion velocity is significantly larger than the 8 km s^{-1} obtained optically by Jeske (1986). We believe that the combination of the two-dimensional nature of our fit and the high-velocity resolution of our observations makes our measurement more reliable.

In Figure 8 we also present the channel maps of the H I observations. In the rest frame of the galaxy, the channel separation is 22.66 km s^{-1}. H I emission from the VII Zw

[4] We caution that we have assumed that the ring is an intrinsically circular structure and that its elliptical shape is entirely a result of an inclined viewing angle. We acknowledge that in models of off-center ring formation, in the early expansion stages, the ring is somewhat noncircular. This may lead to an overestimation of the inclination of the ring and would require a more complicated treatment of the kinematic data.

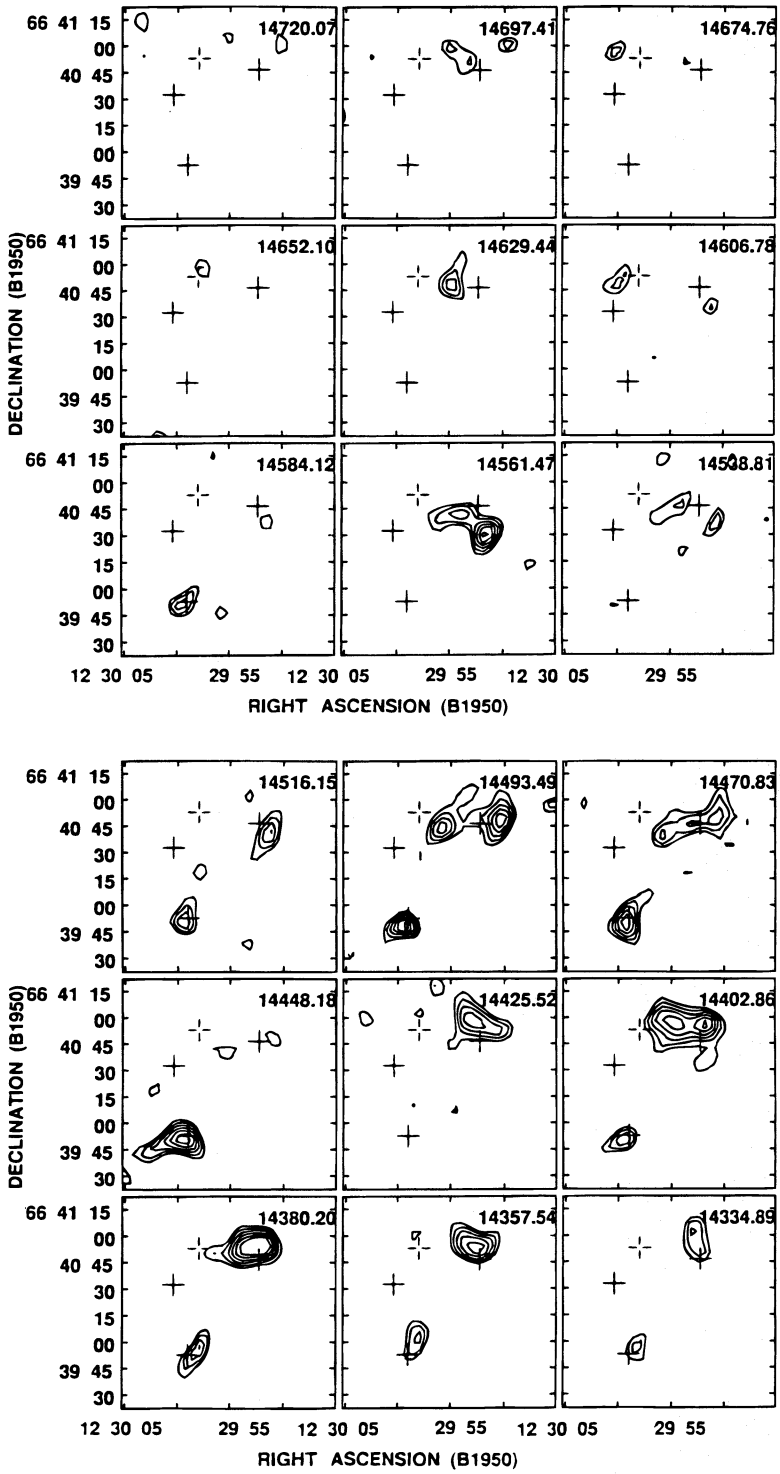

FIG. 8.—Contour plots of the 27 channel maps of VII Zw 466. The velocity of each channel is displayed in the upper right corner. The contour increment is 1.35 × 10^{-4} Jy beam^{-1} (0.5 σ level), and the lowest contour displayed is at 2.5 σ. The filled crosses indicate the position of the ring, G1, and G2, while the open cross indicates the position of the background galaxy B1.

466 is detected for the first time around 14,561 km s^{-1} and originates from the southern side of the galaxy. As we move to lower velocities, the emission is typical of a rotating ring. We observe that the emission splits in two centroids located to the east and west of the optical ring. However, the eastern centroid does not overlap spatially with the optical picture of the ring. It resides at the outside of the optical ring structure and at 14,470 km s^{-1} is deformed into a small plume (hereafter "Plume A") pointing to the southeast. The amount of H I gas associated with this plume is $M_A = 1.6 \times 10^8 M_\odot$. The emission from the western centroid does coincide with the optical ring. It is also considerably stronger, indicating large quantities of gas. Strong emission from the west side of the ring was also detected in the radio continuum observations of the galaxy (Ghigo & Appleton 1996).

As we proceed to channel maps with velocities below 14,470 km s^{-1}, the behavior of the gas is very disturbed.

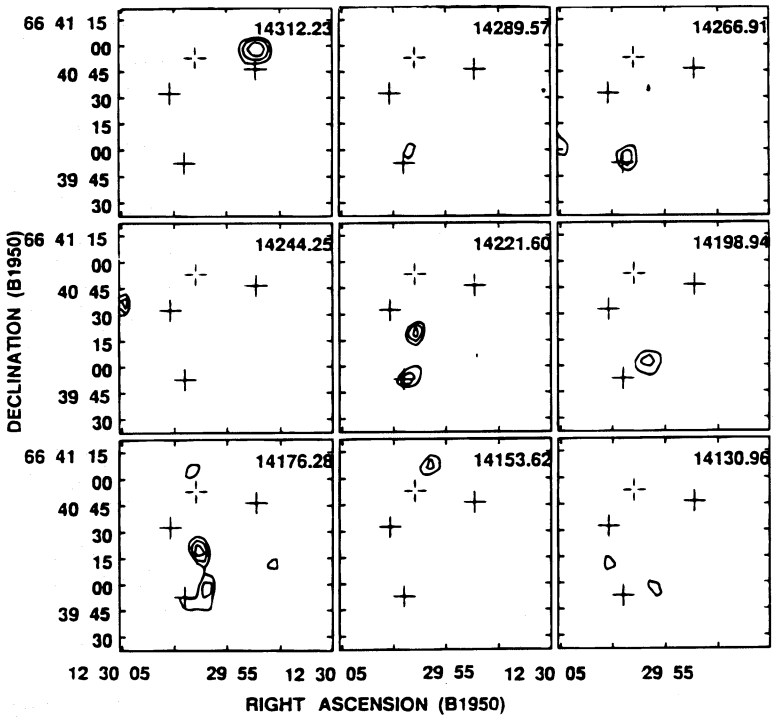

FIG. 8.—*Continued*

First, we notice that at 14,448 km s^{-1} there is practically no H I gas associated with the ring. This is very peculiar since there is a strong emission in the preceding and following channel maps. Also, there is a filament (hereafter "Plume B") of H I gas present in three consecutive channel maps (14,402–14,357 km s^{-1}). This is the strongest emission that we observe. The filament initially points to the northeast of the ring and as we progress to lower velocities, it points to the east-southeast of the ring in the general direction of the companions G1 and G2. We calculated that the H I gas associated with plume B is $M_B = 4.2 \times 10^8\ M_\odot$.

At this point, it also useful to discuss the H I emission from the companion G2. The emission from G2 is located in the channel maps between 14,516–14,334 km s^{-1}. However, we notice H I gas at a velocity of 14,584 km s^{-1} and a lack of H I gas at 14,425 km s^{-1}. Moreover, the emission centroid from G2 in the channel maps after 14,425 km s^{-1} is rather elongated pointing clearly toward the ring galaxy. Table 1 shows that the value of M_{HI}/L_R for G2 is also unusually low for a late-type spiral, suggesting that it has been tidally stripped. (We also note that the total mass-to-light ratio of G2 is extremely low, implying that the dark matter halo of G2 has also been stripped).

The dynamical behavior of the H I gas is consistent with G2 being the galaxy that disturbed the progenitor H I disk of VII Zw 466 and caused the formation of an expanding star forming ring. Numerical simulations of the gas-dynamics of a nearly head-on collision between a large gaseous disk galaxy and a smaller companion disk galaxy (Struck 1996a, 1996b; see also § 8) show that large quantities of gas are stripped away from the disk of the target galaxy by the companion during the collision. Most of the ejected material either falls back to the large disturbed disk or it spirals toward the smaller companion, which eventually accretes it. We will argue that the asymmetric nature of the H I distribution around G2 is strongly suggestive of the onset of accretion from one such tidal stream.

Plumes A and B and emission that extends from the southern end of VII Zw 466 (see Fig. 2) probably form part of a two-horned H I bridge between VII Zw 466 to G2. This rather special morphology is predicted by the models and strongly suggests that the plumes are splattered debris from the collision. The total amount of H I gas in plumes A and B is $M_A + M_B = 5.8 \times 10^8\ M_\odot$, which is approximately 16% of the mass of the H I disk of VII Zw 466. A more detailed discussion of the formation of these structures is given in the next section.

To further estimate the energy needed to generate the two H I plumes, we performed an order-of-magnitude calculation of the kinetic energy of the gas in the plumes. We used the H I masses given above and the relative velocities of plumes A and B $\Delta v_A = 14$ km s^{-1} and $\Delta v_B = 88$ km s^{-1} with respect to VII Zw 466. The kinetic energy associated with their gas was found to be $KE_A = 3.1 \times 10^{53}$ ergs and $KE_A = 3.2 \times 10^{55}$ ergs, respectively. Although projection effects are not included, this implies the energy required to displace the plumes from VII Zw 466 is of the order of 10^{55} ergs. This is approximately 10% the gravitational potential energy of the VII Zw 466-G2 pair, indicating that the collisional scenario is plausible.

7. THE POSSIBLE ROLE OF THE ELLIPTICAL COMPANION G1

In our discussion so far we presented evidence in favor of the edge-on disklike companion G2 as the most likely intruder galaxy. Can we completely rule out the possibility that G1, the brighter elliptical galaxy, is the galaxy that plunged through the center of the progenitor disk of VII Zw 466? After all, an inspection of Figures 1 and 2 shows that the elliptical system lies closer to the minor axis of the ring,

is slightly closer to the ring (2.5 rather than 3 ring diameters away) and has been shown to have peculiar optical isophotes (Appleton & Marston 1995). In addition, its optical velocity (though poorly known) differs from the ring velocity by over 350 km s^{-1}, suggesting a high impact velocity with respect to the ring.

Although we cannot completely rule out the possibility that the elliptical galaxy is the intruder galaxy, we believe the evidence at present is against it. First, all our simulations to date lead to the formation of an accretion stream, which is a bridge between the two galaxies involved in the collision. In the only similar 21 cm H I study so far published, the same behavior is found for the Cartwheel galaxy, where a long H I streamer connects the Cartwheel to its most distant disk companion (Higdon 1996). The fact that the elliptical system is not connected to the ring, nor shows any evidence for H I down to a low column density (see Table 1), seems to rule out accretion of cool gas onto galaxy G1. A careful analysis of the color map of the VII Zw 466 system (see AS96) seems to rule out any evidence for a dusty disk inside G1, similar to those seen in other ellipticals in which accretion is believed to be taking place (e.g., Sparks et al. 1985). Is it possible that any accreting gas might have become ionized? If so, such emission must be weak, since imaging in Hα by Marston & Appleton (1995) failed to show any evidence for ionized hydrogen. In addition, unpublished radio continuum maps of the system by Ghigo & Appleton (1996) show that both VII ZW 466 and G2 are strong radio emitting objects at a wavelength of 6 cm, but that no emission is observed from the elliptical galaxy G1. Similarly, Thompson & Theys (1978) found comparably blue colors in VII Zw 466 and G2, but not in G1. These points again suggest that G1 is a rather inactive object and probably has not suffered accretion recently.

Perhaps the strongest arguments in favor of G1 being the intruder relates to the position of the galaxy relative to the minor axis of the ring and its high relative velocity compared with the ring.[5] The galaxy G1 is only a little closer to the ring than G2, and so from this point of view neither is favored. *N*-body simulations by Huang & Stewart (1988) and Appleton & James (1990) show that very respectable rings can be generated in collisions of quite low inclinations between the intruder and the target disk, reducing the need to always find the intruder close to the minor axis of the ring in all cases. Even the high relative velocity is not a strong argument for identifying G1 as the intruder. Again *N*-body simulations of ring galaxies (e.g., R. A. James 1995, private communication) show that moderately unbound collisions are turned into bound systems via dynamical friction and that it is likely that the relative velocity of the intruder would be significantly reduced after it has travelled a few ring diameters from the target (as observed). In conclusion, we believe that the H I data provide strong evidence that the disk galaxy G2, rather than the elliptical G1, is the likely intruder in this system.

8. MODELS

The H I distribution of Figure 2 suggests that we are witnessing the messy aftermath of a collisional splash between two galaxies. We present here a numerical simulation that supports this picture and provides further details about the dynamics. The model presented here is not a detailed model of this particular system, but it should be viewed as a working example of how the collisional scenario (disk plus disk collision) can produce much of the observed structures. Until higher resolution H I observations are available, a more detailed model that tries to fit all aspects of the system perfectly is not yet justified. The model presented here is part of larger program of simulations between two gaseous galaxy disks. Some preliminary results have been presented in AS96 and Struck (1996a), and a journal paper on these simulations is in preparation (Struck 1996b).

The simulation code is described in the above references, and an earlier version is discussed in Struck-Marcell & Higdon (1993). In this code, the large-scale collision dynamics are modeled within the restricted three-body approximation, which is adequate for the early transient stages of galaxy collisions (e.g., Gerber & Lamb 1994). In these models each galaxy consists of a rigid halo and a gas disk. The potential of the primary galaxy is such as to give a rising rotation curve, which becomes nearly flat at large radii and extends to several disk diameters. A simple softened, point mass form is used for the companion potential. The gasdynamics is computed with a smooth particle hydrodynamics (SPH) algorithm with a spline kernel. In addition to the force from the large-scale potential, a local self-gravity is computed between neighboring gas particles within the disks, which allows the formation of clumps or clouds. Shear dominates over local gravity on scales larger than that on which the latter is calculated.

Simple models for heating and cooling are also included in this simulation. However, isothermal comparison runs show that the large-scale morphology is little affected by these terms (see Struck 1996b for details). The most important result of including these terms, for present purposes, is that the simulations show a prompt, adiabatic cooling of bridge material.

The two disks were initialized in centrifugal balance, with the companion set several primary-disk diameters from the target, and with a slight sideways velocity to allow a slightly off-center impact. The *x*-*y* plane is the initial midplane of the primary disk, while the companion midplane lies on a translated *y*-*z* plane. The companion orbits in the *x*-*z* plane. There is sufficient time before impact for the heating/cooling terms of both disks to reach a quasi-equilibrium.

At the time of impact, extremely strong shocks form. A good deal of primary material is splashed out, so that the bridge ultimately contains a fairly even mix from both progenitors. Similarly, much gas from the companion is left behind. Although this simulation was not specifically produced to model VII Zw 466, the model and time step shown in Figure 9 were chosen as a reasonably good match. In a comparison model using a gasless companion but otherwise identical parameters to the current model show that no gas bridge was formed and little gas debris was ejected from the gas disk. Thus, we see that collisional hydrodynamics (especially a gas on gas collision) seems to plays a key role in the formation of the double-horned H I bridge, in contrast to bridges formed in prograde, planar interactions (e.g., Toomre & Toomre 1972). VII Zw 466 is apparently an interesting example of such a highly dissipative gasdynamical collision.

Figures 9*a* and 9*b* give two orthogonal views of the system some time after impact, when the companion has

[5] Indeed, although Theys & Thompson (1978) seemed to favor G2 as the intruder based on color evidence, they could not rebut this argument in a convincing way (They appealed to three-body effects).

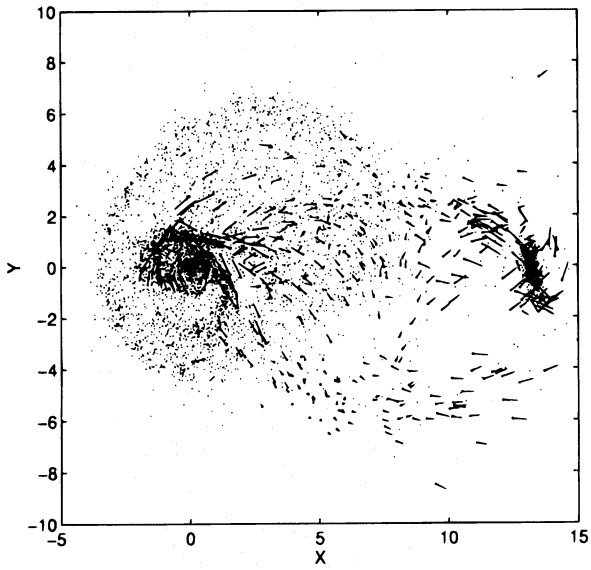

FIG. 9*a*

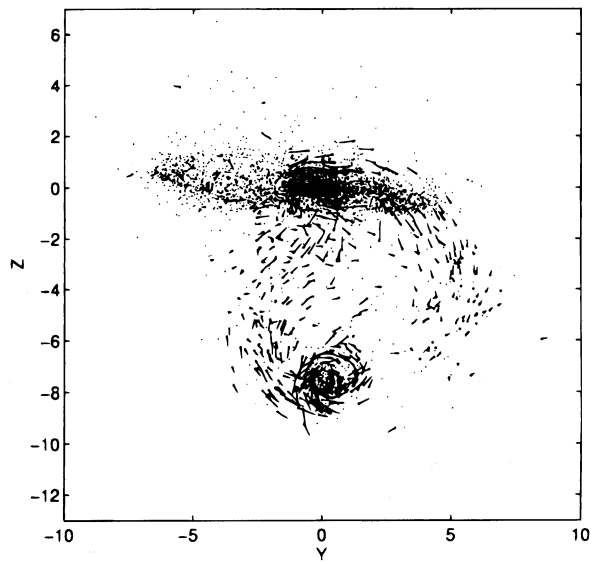

FIG. 9*b*

FIG. 9.—Two orthogonal views of a single time step in a numerical hydrodynamical model of the collision between two galaxies with gas disks. (*a*) *x*-*y* plane, the initial midplane of the primary disk; companion is seen edge-on at right. (*b*) *y*-*z* plane, the initial plane of the companion, now seen at the bottom. Both frames optimized to illustrate the accretion streams. Only 20% of the 19,640 particles in the primary disk, and 50% of the 3240 particles in the companion are plotted. Line segments proportional to the projected direction and magnitude of the velocity of selected particles, with the particle plotted at the base, reveal the flow. The selected particles include all particles originating in the companion galaxy, with temperatures of less than 10 times the initial temperature (i.e., less than 30,000–50,000 K), and located more than 0.5 (dimensionless) units from the $z = 0$ plane. See references in text for further details.

moved a good distance away, with a prominent bridge stretching between it and the primary. We have not attempted to find an optimal viewing angle for the model, though it appears that one about halfway between the two orthogonal views would be quite good. In any case the morphological similarities between Figures 2 and 9 are quite strong. First of all, both have a similar double-horned bimodal appearance, or alternately, a central hole in the bridge material. Animated views of a sequence of model time steps provide a simple explanation. The ring galaxy itself is produced by first an inward gravitational impulse followed by a centrifugal rebound. The same kinematics occurs in the bridge material, with the addition of stretching between the galaxies. Thus, in this picture the bridge is essentially a ring stretched the vertical direction, or a cylindrical annulus.

Figures 9*a* and 9*b* also shows the pattern of infall onto the two galaxies. In the case of the primary disk there is significant infall out of both streams, and the accretion tends to be concentrated in the central regions. In the case of the companion the (highly supersonic) accretion out of one stream is much stronger than the other, though the details are quite time dependent. In both cases the accretion streams swirl around the nucleus and then merge into the ambient rotational flow. Figure 9*a* shows that gas swirls out a relatively large distance on the side opposite the main stream, which may account for the H I asymmetry of G2 in Figure 2. The models indicate that the accreting material is shocked after circling nearly all the way around the companion, and there is much hot and warm gas concentrated on the main stream side. The companion is a radio continuum source, and the models predict that this emission would be offset from the galaxy center if it arises from such shocks. This is in fact observed (Ghigo & Appleton 1996). In the model, the companion disk is highly disrupted in the collision and largely reforms in the accretion process. Although we have no direct evidence for accretion onto VII Zw 466 itself, we note that the large circular loop seen at optical wavelengths in the northwest quadrant of the ring might be the result of bridge material falling back onto the disk. Such material might induce star formation in a ring, which is consistent with Hα observations of the loop (Marston & Appleton 1995).

In an offset collision, the primary disk receives an azimuthal swing impulse as well as the radial one. This leads to asymmetric and offset spatial distributions as seen in both Figures 2 and 9*b*. Figure 9*b* also shows a developing oval ring rather like that in VII Zw 466. This is deceptive, however, since it is the second ring in the model, with the first ring moving out of the disk. At present there is no independent evidence to suggest that the ring in VII Zw 466 is not the first. Thus, it appears that the impact velocity in VII Zw 466 was high relative to orbital or epicyclic speeds in the primary disk, because the companion has moved several ring diameters. The model shows a similar morphology with the first ring, but the bridge has hardly developed at that time. With the aid of kinematical constraints from higher resolution observations at 21 cm, future models for this system should be able to resolve this timing problem and provide more specific predictions.

9. CONCLUSIONS

In the previous sections we presented our H I observations of the VII Zw 466 group. Though only at moderate resolution because of the large redshift ($z = 0.048$) of the group, we were able to draw the following conclusions:

The H I emission from VII Zw 466 is consistent with that of a rotating and expanding ring. A simple kinematical model fits the ring sufficiently well and indicates a rotation curve with $v_{max} = 137$ km s^{-1} at the radius of the ring, and an expansion velocity $v_{exp} = 32$ km s^{-1}. However, one

quadrant of the ring has anomalous velocities and is associated with disturbed H I outside the ring.

The northern part of the ring shows evidence of the tidal interaction. Plumes of H I gas ($5.8 \times 10^8\ M_\odot$, or 16% of the total H I disk) lie outside the ring and point in the general direction of the two nearby group members. The dynamics of this gas is consistent with a collisional origin for the ring. Of the two nearby companions, only the edge-on spiral, G2, contains neutral hydrogen above our detection limits. Its H I properties are abnormal. Not only does G2 exhibit a plume that points toward the VII Zw 466, but it also has very low values of $M_{\rm H\,I}/L_R$ and M_d/L_R. This strongly suggests that G2 is the intruder galaxy that collided head-on with VII Zw 466 and created the ring (Lynds & Toomre 1976). We conclude that the elliptical galaxy G1 has played little role in the ring formation, despite its unusual "boxy" optical isophotes (Appleton & Marston 1995).

Models suggest that the plumes represent a mixture of gas ejected from the progenitor of the ring galaxy and material stripped from the suspected intruder galaxy. The hydrodynamical models provide a good match to the plume morphology and suggest that accretion onto both galaxies is already underway. The models also suggest the possibility that the companion disk was strongly disturbed in the collision, and that the observed asymmetries are the result of partial reformation of the (G2) disk in the accretion process. We identified two new members of the extended VII Zw 466 group. These galaxies are dwarfs and are detected for the first time in H I.

An upper limit to the dynamical mass of the group was estimated using two different techniques and was found to be in the range $M_o = 3.5$–$6.2 \times 10^{12}\ M_\odot$. Adopting the lower end of the range as being more reliable, this implies that the dark matter not associated with the group members is 10 times greater than the sum of the dynamical masses of all group members. The resulting mass-to-light ratio for the group is $(M/L)_{\rm group} \approx 70$.

The estimated M/L for the group is roughly a factor of 3 times lower than the median M/L for loose groups, but is similar to that estimated for compact groups of galaxies. As with compact (Hickson) groups, the low M/L ratio may imply that the group is not in equilibrium, but may be collapsing. Such a scenario would naturally give rise to an increased incidence of deeply penetrating orbits and might increase the probability of a head-on collision leading to the formation of a ring galaxy.

We note that, if the numerical models are correct, the gas plumes seen in these H I observations may represent only a part of the debris formed as the intruder collided with the disk of VII Zw 466. If the collision was quite recent (as implied by the fact that only one ring is seen in VII Zw 466—see AS96 for review), then it is possible that much of the shocked gas accreting onto the two galaxies is still strongly ionized. Deep Hα observations or high-sensitivity UV or X-ray observations may be fruitful.

The authors would like to thank R. J. Lavery (Iowa State University) for stimulating discussions on general galaxy interactions, and J. J. Eitter for instrumentational support at the Fick Observatory. The authors are grateful to an anonymous referee for helpful comments on the manuscript. We are also grateful to E. Brinks (NRAO, Socorro) for useful suggestions during the VLA data reduction process. This work is funded under NSF grant AST 93-19596.

REFERENCES

Appleton, P. N., & James, R. A. 1990, in Dynamics and Interactions of Galaxies, ed. R. Wielen (Berlin: Springer), 200
Appleton, P. N., Kawaler, S. D., & Eitter, J. J. 1993, AJ, 106, 1973
Appleton, P. N., & Marston, T. 1995, preprint
Appleton, P. N., & Struck-Marcell, C. 1996, in Fund. Cosmic Phys., 16, 111 (AS96)
Arp, H. C. 1966, Atlas of Peculiar Galaxies (Pasadena: Caltech)
Bahcall, J. N., & Tremaine, S. 1981, ApJ, 244, 805
Barnes, J., & Hernquist, L. 1992, ARA&A, 30, 705
Butcher, H. R., & Oemler, A., Jr. 1984, ApJ, 285, 426
Dressler, A., Oemler, A., Jr., Butcher, H. R., & Gunn, J. E. 1994, ApJ, 430, 107
Faber, S. M., & Jackson, R. E. 1976, ApJ, 204, 668
Fosbury, R. A. E., & Hawarden, T. G. 1977, MNRAS, 178, 47
Freeman, K. C., & de Vaucouleurs, G. 1974, ApJ, 194, 569
Gerber, R. A., & Lamb, S. A. 1994, ApJ, 431, 604
Ghigo, F., & Appleton, P. N. 1996, in preparation
Jeske, N. 1986, Ph.D. thesis, Univ. California, Berkeley
Hickson, P., de Oliveira, C. M., Huchra, J. P., & Palumbo, G. G. C. 1992, ApJ, 399, 353
Higdon, J. L. 1993, Ph.D. thesis, Univ. Texas, Austin
———. 1996, preprint
Huang, S., & Stewart, P. 1988, A&AS, 197, 14
Jeske, N. 1986, Ph.D. thesis, Univ. California, Berkeley
Landolt, A. U. 1992, AJ, 104, 340
Lavery, R. J., & Henry, J. P. 1988, ApJ, 330, 596
Lavery, R. J., Seitzer, P., Walker, A. R., Suntzeff, N. B., & Costa G. S. D. 1996, ApJ, submitted
Lynds, R., & Toomre, A. 1976, ApJ, 209, 382
Malin, D. F., & Carter, D. 1980, Nature, 285, 643
Marcum, P. N, Appleton, P. N., & Higdon, J. L. 1992, ApJ, 399, 57
Marston, T., & Appleton, P. N. 1995, AJ, 109, 1002
Oemler, A., Jr. 1996, in IAU Symp. 171, New Light on Galaxy Evolution, in press
Ramella, M., Geller, M. J., & Huchra, J. P. 1989, ApJ, 344, 57
Schweizer, F., & Seitzer, P. 1988, ApJ, 328, 88
Sparks, W., Wall, J. V., Thorne, D. J., Jorden, P. R., van Breda, I. G., Rudd, P. J., & Jorgensen, H. E. 1985, MNRAS, 217, 87
Struck, C. 1996a, in Minnesota Lectures on Extragalactic H I ed. E. Skillman (San Francisco: ASP), in press
———. 1996b, in preparation
Struck-Marcell, C., & Higdon, J. L. 1993, ApJ, 411, 108
Theys, J. C., & Spiegel, E. A. 1976, ApJ, 208, 601
Thompson, L. A., & Theys, J. C. 1978, ApJ, 224, 796
Toomre, A., & Toomre, J. 1972, ApJ, 405, 142
Vorontsov-Velyaminov, B. A. 1977, A&AS, 28, 1